The Aeronautical Journal (2022), **126**, pp. 1288–1302
doi:10.1017/aer.2022.28

REGULAR PAPER

Design of a sub-scale fan for a boundary layer ingestion test with by-pass flow

H. Mårtensson[1,*], M. Lejon[1], D. Ghosh[2], M. Åkerberg[2], F. Rasimarzabadi[3] and M. Neuteboom[3]

[1]GKN Aerospace Engine Systems, Trollhättan, Sweden, [2]Chalmers University, Gothenburg, Sweden and [3]National Research Council of Canada, Ottawa, Canada
*Corresponding author. Email: hans.martensson@gknaerospace.com

Received: 26 November 2020; **Revised:** 15 October 2021; **Accepted:** 2 March 2022

Keywords: Distortion; Boundary layer ingestion; Fan

Abstract

A design of a sub-scale Boundary Layer Ingestion (BLI) fan for a transonic test rig is presented. The fan is intended to be used in flow conditions with varying distortion patterns representative of a BLI application on an aircraft. The sub-scale fan design is based on a design study of a full-scale fan for a BLI demonstration project for a Fokker 100 aircraft. CFD results from the full-scale fan design and the ingested distortion pattern from CFD analyses of the whole aircraft are used as inputs for this study. The sub-scale fan is designed to have similar performance characteristics to the full-scale fan within the capabilities of the test facility. The available geometric rig envelope in the test facility necessitates a reduction in geometric scale and consideration of the operating conditions. Fan blades and vanes are re-designed for these conditions in order to mitigate the effects of the scaling. The effects of reduced size, increased relative tip clearance and thicknesses of the blades and vanes are evaluated as part of the step-by-step adaption of the design to the sub-scale conditions. Finally, the installation effects in the rig are simulated including important effects of the by-pass flow on the running characteristics and the need to control the effective fan nozzle area in order to cover the available fan operating range. The predicted operating behaviour of the fan as installed in the coming transonic test rig gives strong indication that the sub-scale fan tests will be successful.

Nomenclature

ADP	Aerodynamic Design Point
BLI	Boundary Layer Ingestion
BPR	By-pass ratio – mass flow in by-pass over fan mass flow
CFD	Computational Fluid Dynamics
Cpt	Coefficient for total pressure, divided by reference total pressure
NRC	National Research Council, Canada
PRts	Pressure ratio, inlet total-to-outlet static
PRtt	Pressure ratio, total-to-total
SLS	Sea Level Static
TCT	Tail Cone Thruster
$\Delta h/U_m^2$	Loading coefficient
C_x/U_m	Flow coefficient

1.0 Introduction

Boundary Layer Ingestion (BLI) technology has the potential to reduce aircraft fuel consumption by improving the propulsion efficiency of aircraft engines. The principles for this have been known for

This paper is a version of a presentation due to be given at the 2022 ISABE Conference

a long time and are described first in [1]. Thrust is generated by adding momentum to the air stream passing through the fan and exiting the nozzle as a jet at a higher velocity. Benefits of BLI stems from the reduction of power needed to increase the momentum of a low velocity fluid to provide the required thrust. Fundamentally, the kinetic energy increase needed to accelerate an airstream is quadratic with the exit velocity, whereas the momentum increase is linear for a given mass flow. Therefore, accelerating low-momentum flow found in the boundary layer to a given jet velocity is less energy consuming than to accelerate the high-momentum freestream air to achieve the same thrust. The air entering the BLI fan in reality consists of a mixed airstream that includes lower momentum flow entering the fan from boundary layers and upstream wakes as well as higher momentum fluid from the freestream. This makes the analysis of the potential benefit more complex and has been the subject of several papers. In [2] and [3] the effects of the distribution of momentum deficit of the ingested air is investigated. In order for the BLI concept to work the fan must be able to work efficiently with the distorted air that is ingested. Fan sectors ingesting the low momentum flow will cause the blade to operate at a higher aerodynamic load passing through the sector resulting in an increased total pressure rise, which gives the desired BLI effect. Provided that the fan rotor does not stall and operates at good efficiency the BLI fan will give a higher propulsive efficiency than what would be the case for the non-BLI fan.

Although the potential benefits are known in general, fan performance and the possibly detrimental effects of ingesting distorted air needs to be better understood. The design of BLI fans are more complicated relative to non-BLI fans (or standard turbofans) since the flow varies radially as well as circumferentially. Published examples of design concepts that have been put forward include symmetric as well as asymmetric BLI designs. A design where the fan ingests the boundary layer asymmetrically across the fan face is the Blended Wing Body configuration. Examples of this also include the D8 4 5 concept and NASA developments studies as summarised in [6]. A conceptually different integration concept is the TCT (Tail Cone Thruster) as used here. The intent of the TCT is to ingest a boundary layer developed around the fuselage as a mainly axisymmetric flow profile. Examples of studies into similar concepts can be found in the NASA study [7] and from the EU project Centreline [8].

Improving the ability to design and analyse BLI fans requires both detailed analytic work as well as experimental data. Some analytic and experimental work on BLI with a rotating fan has already been reported in the literature. In [9], a low-speed, single-stream rig was used to investigate an asymmetric BLI case. In the study, a fan designed for BLI in a TCT configuration was compared to a fan designed for clean inlet conditions. The BLI fan was designed by increasing the loading and solidity at mid span. The tip section was re-staggered in order to accommodate the intermittent incidence increases found in circumferential distortion. A combined low-speed experimental and CFD study was presented in [10] studying the effects of predominantly asymmetric distortion on fan aerodynamics. Important effects on flow re-distribution and an increased loss were shown that resulted from the BLI. A CFD study presented in [10] of a transonic fan found that the behaviour here was similar to the low speed results, with some added complexity due to the complex shock systems. A larger transonic experiment performed in a wind tunnel with a by-pass stream was described in [11]. The installation in this case was asymmetric, with the fan ingesting the boundary layer developed over a surface upstream of the 22-inch fan. The results focused mainly on a detailed investigation of blade vibration. The results showed that the fan sustained testing, but also pointed out the importance of robustness to vibration in view of the long operation time in distortion.

The present study aims at designing and analysing a fan serving as a test object for a BLI research test rig. The broader purpose of the rig built by The National Research Council of Canada (NRC) is to gain an understanding of whether BLI is advantageous in reducing the power required for a given thrust as discussed in [12]. Integrating the fan with the aircraft in order to gain the improvements of BLI, increases the complexity of the fan design, as each possible installation will generate a unique distortion pattern that the fan needs to cope with. The starting point for this study is a design of a BLI fan specifically for the Fokker 100 aircraft [13]. For future developments an understanding of how different distortion patterns affect the design is needed. The objective here is to gain knowledge of how the ingestion of boundary layer flow affects fan performance in a broader sense. The unique features of the rig (as shown in Fig. 1), lies in the ability to adapt the inlet flow and to operate the fan at varying conditions. The

https://doi.org/10.1017/aer.2022.28 Published online by Cambridge University Press

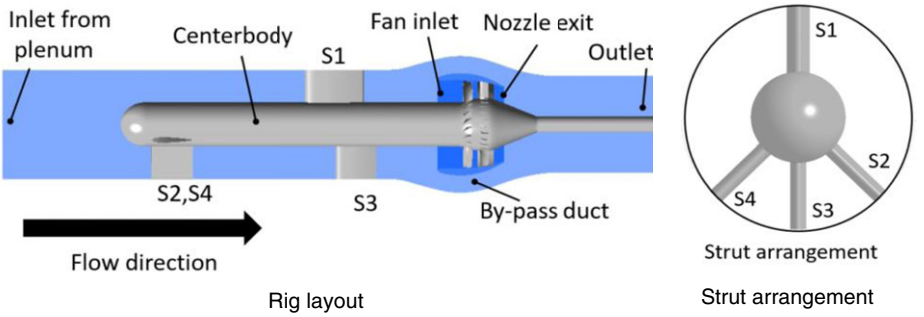

Figure 1. *Overview of rig cross section.*

fan operating point can be varied with the use of blocker plates in the nozzle in addition to variations controlled by the rig pressure ratio. Modifying the centerbody to thicken the boundary layer, or wakes, affects the incoming flow distortion directly.

The fan will operate at high speed in transonic conditions in a wind tunnel with a by-pass stream. Using the versatility of the rig, different levels and patterns of distortion can be generated for knowledge building and validation. The BLI distortion pattern used as a baseline includes both an axisymmetric radial variation as well as circumferential features stemming from the aircraft as described in a BLI fan study applied to a Fokker 100 12. In Fig. 1a the layout of the rig is shown with axial positions of the struts shown in the cross section along with the fan and by-pass duct. The strut arrangement is further shown in Fig. 1b, where struts S1 and S3 create distortion in the circumferential positions of the vertical tail and the struts S2 and S4 represent the engine pod wakes.

Following the design and analyses made with the fan stage using the conditions derived from the full scale, the sub-scale fan stage design is introduced into a model of the whole test rig. CFD analyses are then performed in order to understand how the fan and rig will perform together.

2.0 Design of the sub-scale fan

The purpose of the sub-scale design is to develop a test object that is representative of a BLI fan for an aircraft. The design is done using similarity conditions that approximate those of the full design. The reduction in scale involves adapting the design to the geometric scale and conditions that can be reproduced in the test facility. The geometric size as well as the limited available power, makes it necessary to adapt the design. For a BLI fan mounted on the tail cone the incoming flow is characterised by distortion that is given by the flow developing around the aircraft. The fan design will therefore need to be mechanically robust as well as aerodynamically tolerant to variations in operating conditions. Design conditions for the sub-scale fan are derived from the BLI fan integrated with a Fokker 100 aircraft as described in [14] and [12].

The ADP (Aerodynamic Design Point) is a central operating point in the design as it is representative of most of the flight time. Since this is the operating point where most energy is consumed by the aircraft, good efficiency is desired. The ADP for this case corresponds to Mach 0.74 and an altitude of 35000ft. Table 1 gives the main characteristics of the full-scale fan and the scaled design at ADP. The scaled fan conserves the corrected tip speed, which results in a similar tip Mach number, which is an important characteristic number for a transonic design. The Reynolds' number on the other hand is considerably lower in the sub-scale fan. While the Reynolds number is $1.3 \times 10^6$for the full-scale fan based on rotor mid-span chord, it is 1.3×10^5 for the sub-scale fan. This is a consequence of the reduced chordal dimension as well as a reduced pressure level in the rig. Operating the rig at 24 kPa reduces the power needed for driving the fan to match the available motor power, but results in low density which coupled

https://doi.org/10.1017/aer.2022.28 Published online by Cambridge University Press

Table 1. *Principal design data from the full scale used for the sub-scale design.*

	Full-scale Fan ADP	Sub-scale Fan Design Condition
Tip diameter, D	1.2 m	0.18 m
Shaft speed, N	4419 rpm	32080 rpm
Corrected tip speed	302 m/s	302 m/s
Mass flow	46 kg/s	0.75–0.79 kg/s
Reynolds' number, based on rotor mid-span chord	1.3×10^6	1.3×10^5
Total pressure ratio, $\boldsymbol{PR_{tt}}$	1.3	1.27–1.30
Average total pressure at fan face, $\boldsymbol{P_{t,2}}$	29 kPa	24 kPa
Total temperature at fan face, $\boldsymbol{T_{t,2}}$	243 K	288.15 K
Flow coefficient, $\boldsymbol{C_x/U_m}$	0.73	0.69
Loading coefficient $\boldsymbol{\Delta h/U_m^2}$	0.5	0.5
Isentropic efficiency design target	>0.90	>0.80
Number of blades and vanes	18, 46	18, 24

with the smaller dimensions produces a Reynolds number an order of magnitude lower than the full-scale design. The adaption to a smaller geometric scale makes it necessary to allow for some variation in the performance parameters relative to the full-scale fan.

The flow path annulus from the fan face to the nozzle of the sub-scale fan is similar in shape to the full scale but with a uniform reduction in geometric scale of axial and radial coordinates, whereas the blade profiles were adapted when scaled to the smaller size. The main changes necessary are thicker blades and a larger tip clearance relative to the blade span. As a consequence, increased losses and increased geometric blockage of the flow path are anticipated. It was therefore deemed appropriate during the sub-scale fan design effort to allow a design tolerance on the mass flow to be 5% lower than what an equivalent flow coefficient would give, and the pressure ratio 0.03 lower than the full-scale values as shown in Table 1. The design aimed to recover efficiency as much as possible, targeting an isentropic efficiency above 80%, while still within the tolerance on pressure ratio and mass flow.

2.1 Inlet boundary condition for the sub-scale fan design

The tail cone mounted fan ingests the primarily axisymmetric boundary layer that has developed over the fuselage; however, it will experience wakes from the vertical tail plane and main engine pods. The flow ingested by the full-scale fan is shown in Fig. 2b, where the radial as well as the circumferential distortion components are visible. Data for this are taken from the CFD analysis of the whole Fokker 100 aircraft including the TCT. Figure 2 shows the distribution over the fan face (b) and the circumferentially averaged radial profile (a) derived from the same data set as used in [12]. In addition to providing good performance at ADP, the TCT is required to operate while the aircraft is on the ground where an absence of ram pressure pushes the fan working line towards stall. At ground static conditions the boundary layer does not develop in the same way over the fuselage. For the ground static case the inlet total pressure distribution was simplified as a uniform constant value.

The sub-scale design calculations considered only the fan blade and vane, and applied the full-scale inlet boundary total pressure profile as shown in Fig. 2a. A similar pressure ratio to the full-scale design was also applied. In addition to this condition referred to as "BLI Profile" a second inlet condition referred to as the "Flat" inlet condition was used to represent an inlet flow similar to that ingested at static conditions. The "Flat" profile was implemented simply by imposing a uniform total pressure over the fan inlet. In both cases the total temperature at the inlet is constant at 288.15 K. For each of these inlet conditions, a sequence of back pressures was applied to the nozzle in order to generate a full-speed line. The intent was to simulate operation over widely different test conditions and to confirm the robustness of the fan.

https://doi.org/10.1017/aer.2022.28 Published online by Cambridge University Press

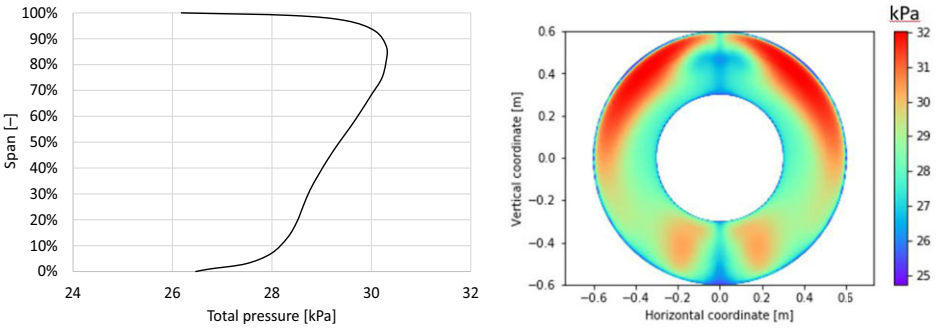

Figure 2. *Full-scale total pressure at inlet (a) circumferentially averaged per span (b) over the inlet to the fan.*

2.2 Sub-scale fan blade and vane re-design

As mentioned previously, some modification to the full-scale blade profiles was required when designing for the smaller scale fan. Profile thicknesses, as well as leading and trailing edge radii on a transonic fan are normally very small in order to maximise performance. These geometric dimensions are too small to be practically scaled to the smaller size as they would become too small to manufacture. The design philosophy placed priority on ensuring that the blades and vanes could be manufactured with good precision to the intended geometry while being mechanically robust. Because the order of scaling is significant, and the practical limitations on leading edge and trailing edge thickness are so limiting, the ratio of the leading and trailing edge thicknesses relative to the chord are much larger in the sub scale design than the full-scale design. This increased ratio results in compromised efficiency. Similarly, the tip clearance relative to the blade span is increased on the sub-scale design. Consequently, the blades were re-designed to recover some of the performance lost due to the blockage and losses of the thicker aerofoils.

A performance stack up of the various deviations from the original fan design is shown in Table 2. The same boundary conditions at inlet and outlet were used for all design iterations. A constant total temperature and the radial profile of total pressure shown in Fig. 2 are prescribed at the inlet, while an average static pressure is specified at the outlet. A large number of design iterations were made in order to find the geometries for cases number 3 and number 5 in Table 2. These CFD simulations were performed on design meshes using the k-ϵ turbulence model with wall functions in ANSYS CFX 2020R1. The results should be interpreted carefully as the model used was not adapted for very low Reynolds number flows but is expected to provide guidance for design choices. In a later section of this paper, the final design is analysed using higher fidelity CFD models, including transition modelling.

The first step of the re-design process, shown as case 1 in Table 2, was done to compare the performance of the scaled down model to the full-scale geometry at similarity conditions for both Mach and Reynolds number. This step was made to check that the geometric downscaling was done accurately for the CFD model geometry. The scaled down model forms the reference in the stepwise development of the sub-scale fan design.

A consequence of the scaling in the aerodynamic tests is a reduction in Reynolds number which for this rig is an order of magnitude lower compared to the full-scale design. This is evaluated in case 2, where a modest reduction of the flow range as well as a 2% reduction in efficiency was seen.

The next step, case 3, takes into account the change of relative thickness imposed by manufacturing limitations. Transonic fan blades tend to be thin, in particular with very small leading and trailing edge radii, which presents challenges to manufacturing at a smaller geometric scale. For the scaled down transonic fan blades a leading and trailing edge minimum radius of 0.35mm was imposed. The blade

https://doi.org/10.1017/aer.2022.28 Published online by Cambridge University Press

Table 2. *Efficiency changes due to scaling to experimental rig size.*

Sub-scale Design Cases	Incremental Efficiency Change	Accumulated Eficiency Change $\Delta\eta_p = \eta_{p,case} - \eta_{p,ref}$
1. Scaled model at ADP similarity conditions, ref		0.0%
2. Scaled model test rig conditions, Re change	−2.0%	−2.0%
3. Increased thickness	−6.3%	−8.3%
4. Increased tip clearance from 0.6% to 1.2% of leading-edge span	−1.9%	−10.2%
5. Reduced stator count from 46 to 24 vanes	+2.9%	−7.3%

is further made robust by designing a blade that is thick, in particular in the root section relative to the original design. This keeps the stresses low and the frequencies of the lower modes high, reducing the risk for a blade failure. The final design has a root thickness that is 15% of the chord giving a first bending mode frequency above the third engine order at full speed. As a consequence, changes were made in order to accommodate the design aerodynamically with as small impact as possible on the performance. The design work includes changes to the blade shape intended to keep performance as close to that of the original design as possible. Profile curvatures and slopes are therefore changed at the same time as the areofoil thickness distribution.

The change in airfoil thickness is shown in Table 2 (case 3) has the largest impact on efficiency compared to the other steps in the design, reducing efficiency by 6.3%. Combined, the change in Reynolds number and increased thickness reduce efficiency by 8.3%.

For the original fan, the tip clearance was set as 0.6% of the span. However, for the scaled-down model this results in a tip clearance which is too small to manufacture and operate reliably. Case 4 introduces a tip clearance of 0.5mm, which corresponds to 1.2% of the span. This step is shown to reduce efficiency by 1.9%. The change in efficiency that result from a change in tip clearance size depends on a large number of parameters e.g. blade loading, flow coefficient, solidity, stagger angle and location along the speed line as described in [15]. While an efficiency loss of 1.9% is relatively high for this change in tip clearance size, it is in line with performance loss reported in earlier work when the tip clearance size was varied for a transonic compressor rotor [16]. One factor for increased losses in case 4 could be the increased loading towards the tip in this case, as the total pressure profile at the inlet is biased towards the higher radii, but this was not investigated in detail.

The cumulative change in efficiency from the change in Reynolds number, increase in thickness and tip clearance size, is thus 10.2%.

The final step, case 5, was to reduce the vane count from the 46 used in full-scale to 24 in the design for the rig in order to keep a reasonable shape of the vanes and to improve manufacturability of the vanes. The change in vane count is done while conserving solidity which results in a larger chord. This step is shown to re-gain some of the lost performance having a net positive impact on efficiency of 2.8%. The change in efficiency, when comparing the original full-scale design to the sub-scale model suitable for rig test, is a reduction of 7.3%.

The plots in Fig. 3 illustrate the changes of the profile shapes at mid-span that followed from the major steps in designing the sub-scale fan blades and vanes. Figure 3a shows Mach number contours at mid-span for case 1, which is representative of the flow field for the full-scale model. Figure 3b shows case 3 where thicknesses of blades and vanes are both increased. The scaled blade exhibits a slightly higher Mach number visible on the suction side and a thicker wake. Similarity the full scale is considered acceptable as a result of the thickening of the blade. For the stator shape on the other hand the Mach number increase was difficult to mitigate through modifications of the profile. This leads to a design with

https://doi.org/10.1017/aer.2022.28 Published online by Cambridge University Press

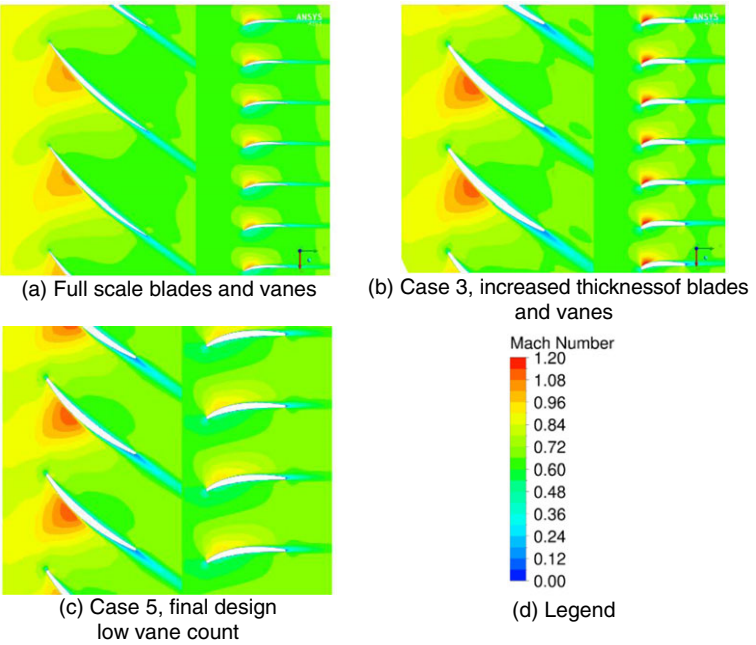

Figure 3. *Mach number plots at mid span comparing full scale and sub-scale results.*

a reduced vane count. Figure 3c shows case 5 where the vane count reduction is introduced in order to recover some loss incurred by the relative thickness increase of the vanes. The plot shows the reduction in relative thickness of the stator resulting from the chord increase, as well as a reduction in suction side Mach numbers.

2.3 Analysis of re-designed blade with prescribed inlet profile

With all changes implemented, the performance of the rig design at design speed was compared to the original design. This was done using a mesh with resolved boundary layers ($y+ < 1$), with the fan blades resolved using a hexahedral structured mesh with 2.8 million nodes per blade passage while the stators are resolved using 1.8 million nodes. The turbulence model used for the analyses of the sub-scale fan design is the k-ω SST turbulence model in ANSYS CFX 2021R1.

Speed lines were calculated with a fixed fan speed and inlet boundary condition. The design point, but also the off-design characteristics, are shown this way. The two main speed lines of the sub-scale model are shown in Fig. 4 as the "BLI Profile", which reflects the main design condition, and the "Flat profile". For the "Flat Profile" the inlet total pressure is simply constant as an idealisation of the conditions that would be relevant for the airplane at static conditions. These inlet profiles are derived from the study of the full scale fan reported in [13]. The "scaled baseline" was taken from the same study but re-normalised for comparison with the sub-scale fan results. While slightly steeper in the sub-scale design the speed lines are sufficiently similar for the design to be considered representative. This may be expected as the blades are thicker relative to the chord which tends to reduce the choke mass flow. A reference point with PRtt=1.30 and a mass flow of 0.76 kg/s at 24 kPa total pressure and 288.15K at the fan face and for the sub-scale fan is included in Fig. 4. In view of the relatively low Reynolds' number, an additional computation is made using the Gamma-Theta transition model available in ANSYS CFX. This simulation uses the same boundary conditions and mesh as the "BLI profile". An increased pressure ratio over most of the speed line is observed while the flow range is largely unaffected which indicates a modest sensitivity in the design.

https://doi.org/10.1017/aer.2022.28 Published online by Cambridge University Press

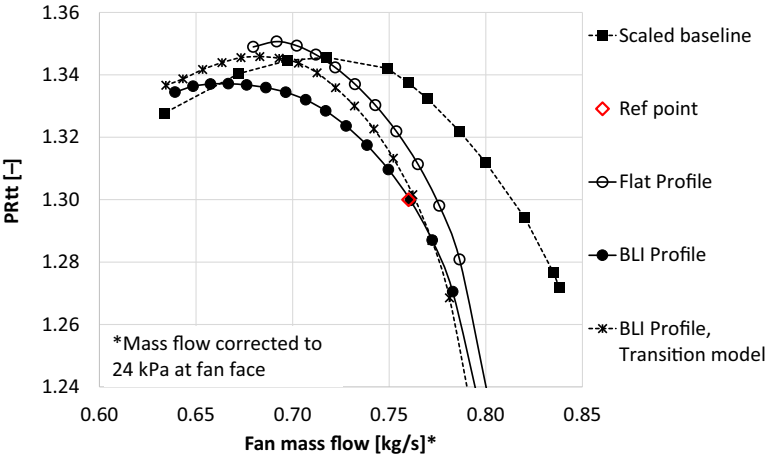

Figure 4. *Speed lines as calculated for the full-scale and rig design.*

The BLI speed line extends to mass flows below the ADP reference point giving some confidence that other conditions will be possible to accommodate in later tests. The lower mass flow end of the "BLI Profile" speed line, is reached at approximately 85% of the mass flow at the reference point. This gives an indication of the stability margin, which is needed in order to ensure that the fan can cope with a variation in operating point in the rig. In addition, the "Flat Profile" speed line extends down to 90% of the reference mass flow. This is taken as an indication that the fan is stable enough to allow for testing of a variety of inlet distortion profiles in test, which is part of the objective for the design.

3.0 Installation effects with by-pass

The sub-scale fan design is intended to be tested in an experimental rig to validate methods used to simulate and to explore the BLI fan performance. With the fan installed in the rig including a by-pass flow as shown in Fig. 1, the characteristics will be different from that in a traditional, single stream rig. With by-pass, the ingested stream tube as described by the by-pass ratio, changes with fan speed as well as with the rig pressure ratio. With the design frozen, the fan function is evaluated using an analysis of the whole rig test section including the fan from inlet to outlet as in Fig. 1. The simulations to map the performance characteristics of the installed fan were performed using sector models of the fan with mixing planes used for the interfaces between rotor, stator and the rig meshes. This permitted the blade and vane rows to be modeled using a single entity for each blade row. The same mesh described in section 2.3 for the fan stage analysis was re-used for the steady state rig analysis.

The CFD results of the full rig were generated using the k-ω SST turbulence model in ANSYS CFX 2021R1. A grid consisting of approximately 4 million cells was used to resolve the flow in the rig upstream and downstream of the fan stage and in the by-pass section. Using this setup, the CFD analysis of the rig becomes very similar to that used in design for the turbomachinery part. The rig parts are modeled in order to have a good representation of the entire test section from inlet to well downstream of the fan. Mixing planes will capture the average radial distribution of the ingested flow, but not to the circumferential variation since mixing planes average out these variations before applying them to the adjacent mesh domain.

In addition to the steady state analysis, a fully transient 360° analysis was performed of the test rig. This includes all 18 blades and 24 vanes resulting in a total of 48 million grid points for the complete computational domain. The transient solution was simulated over a number of revolutions until the flow was periodic. Such analyses are computationally demanding, and therefore a coarser mesh was

https://doi.org/10.1017/aer.2022.28 Published online by Cambridge University Press

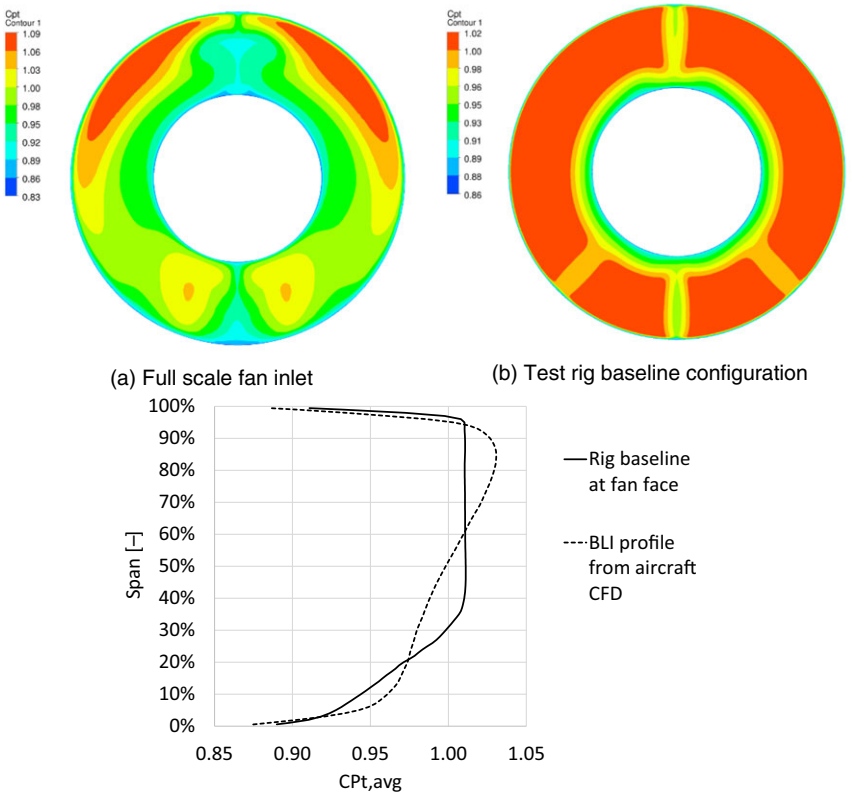

Figure 5. *Total pressure variation over the fan face (a) for the full scale fan design derived from a whole aircraft model [14] (b) at the fan face installed in the rig at the rig reference point.*

applied for the blade rows with about 1.3 million nodes per blade and 0.8 million nodes per vane. The transient analysis complements the steady analysis by capturing the blade-vane interactions as well as the circumferential distortion and how that propagates through the fan system.

3.1 Inlet conditions

The ingested flow pattern will vary in the tests due to the by-pass flow and the different inlet distortions generated. When integrated in the baseline rig the flow entering the fan at design point will differ somewhat from the full-scale flow. Figure 5 shows a comparison of the total pressure distribution at the fan face from the whole aircraft analysis with the baseline configuration to be used in the rig at the reference operating point as shown in Fig. 4. In the rig, a similar basic total pressure distribution is achieved with the visible 6 and 12 o'clock wakes behind the struts representing the vertical tail plane, as well as the wakes behind engine pylons at 4 and 8 o'clock. The pressure deficit due to the wakes in the rig is not as pronounced as it is for the full aircraft. This is intentional as it is relatively easier to add elements to the rig than to remove them. However, the resultant radial total pressure profile derived using a circumferential averaging shows a much less developed rig boundary layer than the for the full aircraft.

In later stages of testing the intent is to increase and vary the distortion. Starting from the baseline test, the flow will be modified along the centerbody creating stronger boundary layers and a variation

https://doi.org/10.1017/aer.2022.28 Published online by Cambridge University Press

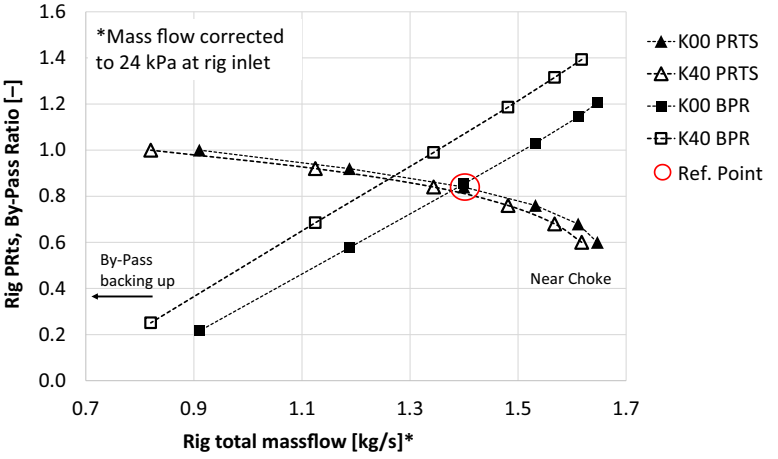

Figure 6. *Rig characteristics and the effect on by-pass for the installed model.*

in blockage. The upstream sections in the long inlet section also offers a flexibility in increasing the thickness of the strut wakes by thickening them.

3.2 By-pass flow

Operating the fan in a rig with a by-pass, or as intended on the tail cone of an aircraft, is different from a single stream installation. The most common set-up is having the compressor or fan installed in a single stream with a tube or bell mouth installed upstream, which is also the way in which the design analyses are done. At the reference point, the inlet flow field can be assumed to be close to what was used in design. Installed on the aircraft the fan operating point will be affected by the ram pressure at different Mach numbers, shifting the working line of the fan. At high Mach numbers, the ratio of total pressure at the inlet to the static pressure at the nozzle is large, lowering the fan pressure ratio. In the case of BLI, the fan will also be affected by the portion of the flow that becomes ingested as the captured stream tube changes, characterised by the by-pass ratio (BPR) in the rig. This is somewhat resembling the effect of the stream tube captured by the fan and the drag over the fuselage that varies with aircraft speed. In the rig a similar role to that of the ram pressure is played by PRts, the ratio of inlet total to outlet static pressure ratio of the whole rig. Varying PRts was done in the CFD model by changing the back pressure at the rig exit, far down stream of the nozzle. Figure 6 focuses on the rig flow as it shows the variation in BPR and PRts as a function of rig mass flow with the fan running at design speed. This reveals some interesting qualities of the interaction with the by-pass flow. The K00 entries refer to the fan installed in the baseline rig. The K40 curve describes the case where a perforated blocker plate is installed in the nozzle. This is set to spoil dynamic pressure in the nozzle, so as to change the effective throttle area sensed by the fan. This purpose for introducing this blocker plate is discussed in later sections of this paper.

The upper mass flow limit of operation is shown in terms of the highest mass flow that can be reached before the flow chokes. The lowest rig mass flow considered useful here gives a BPR slightly higher than 0, and the exit static pressure is almost equal to the inlet total pressure. Around this point, parts of the flow start to recirculate back up through the by-pass, which is also the last point where analyses are made. The total rig mass flow is still positive at this point as the fan raises the total pressure downstream of the nozzle and effectively acts as an ejector pump on the by-pass flow.

Focusing on the ingested flow at increasing BPR (lower rig back pressure), the incoming boundary layer develops a stronger profile due to the increasing losses in the upstream duct. At low BPR, the fan

https://doi.org/10.1017/aer.2022.28 Published online by Cambridge University Press

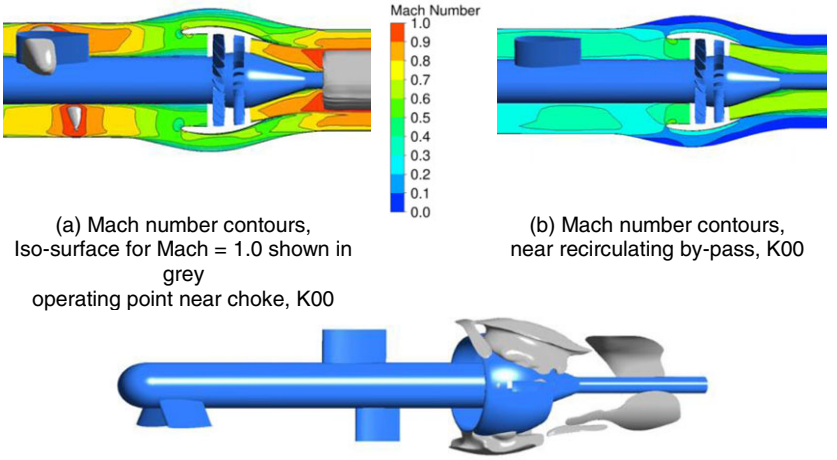

Figure 7. *Flow visualisations showing the contrast between high and low operating points.*

may start to also ingest the boundary layer on the outer annulus of the rig upstream of the fan as the captured stream tube grows.

In order to illustrate the differences between the extremes, Mach number contours at an operating point near choke and near stall of the fan are shown in Fig. 7a and Fig. 7b, respectively. Figure 7a shows the K00 case corresponding to the highest flow point in Fig. 6 which is indicated as close to choke. Iso-surfaces of Mach number =1 are added along with a plane along the symmetry line in order to visualise the 3-dimensional supersonic pockets that form on the struts as the flow rate in the rig increases. The edge of the jet issuing from the fan nozzle is supersonic, spreading slowly, as lower momentum flow from the by-pass is entrained. Figure 7b corresponds to the other end point in Fig. 6 deemed useful in the analyses, where the back pressure increased to the point where back-flow starts to recirculate as shown in Fig. 7c. The Mach numbers are near zero in the by-pass, and the flow is 3-dimensional (Fig. 7c) showing regions of stalled flow. Increasing the back pressure further from this point leads to significant re-circulation from the downstream side to the fan entry, which is not a useful condition for our purposes.

Figure 8 shows the characteristics of the fan installed in the rig together with the fan speed lines obtained with fixed inlet conditions. The entries K00 (open nozzle) and K40 (configuration with nozzle blocker plate) denote the same succession of operating points as in Fig. 6 but now with the fan mass flow on the horiontal axis and the fan stage PRtt (stage total-total pressure ratio) on the vertical. These are overlaid on the fan speed lines from Fig. 3. What is clear is that the K00 speed line, which is the unmodified fan operating at design speed, is much more vertical and limited than the design speed lines. One point of high interest for the test is to explore the fan design to the functional limits. It is likely from the K00 line that the by-pass duct will back-up and reverse before the fan stalls, as the lowest mass flow point is very far from the lower range limit of the design speed lines. In order to move to a lower mass flow with a controlled flow at the fan inlet, to the functional limit, the fan will need to be throttled. The K40 speed line results from installing a blocker plate that spoils some total pressure in the nozzle, thus reducing the nozzle effective area significantly and forces the fan to operate at a higher pressure ratio. Tests conducted with a perforated blocker plate installed will enable operation with higher by-pass ratio for a given rig pressure ratio and mass flow. This will be necessary to preserve the fan inlet pressure profile by alleviating recirculation the by-pass duct when assessing the fan performance near the stall line.

For reference the speed lines denoted “Flat profile” and “BLI Profile” as shown in Fig. 4 are added to Fig. 8. The speed lines are generated with a total pressure profile at the inlet that is independent of the

https://doi.org/10.1017/aer.2022.28 Published online by Cambridge University Press

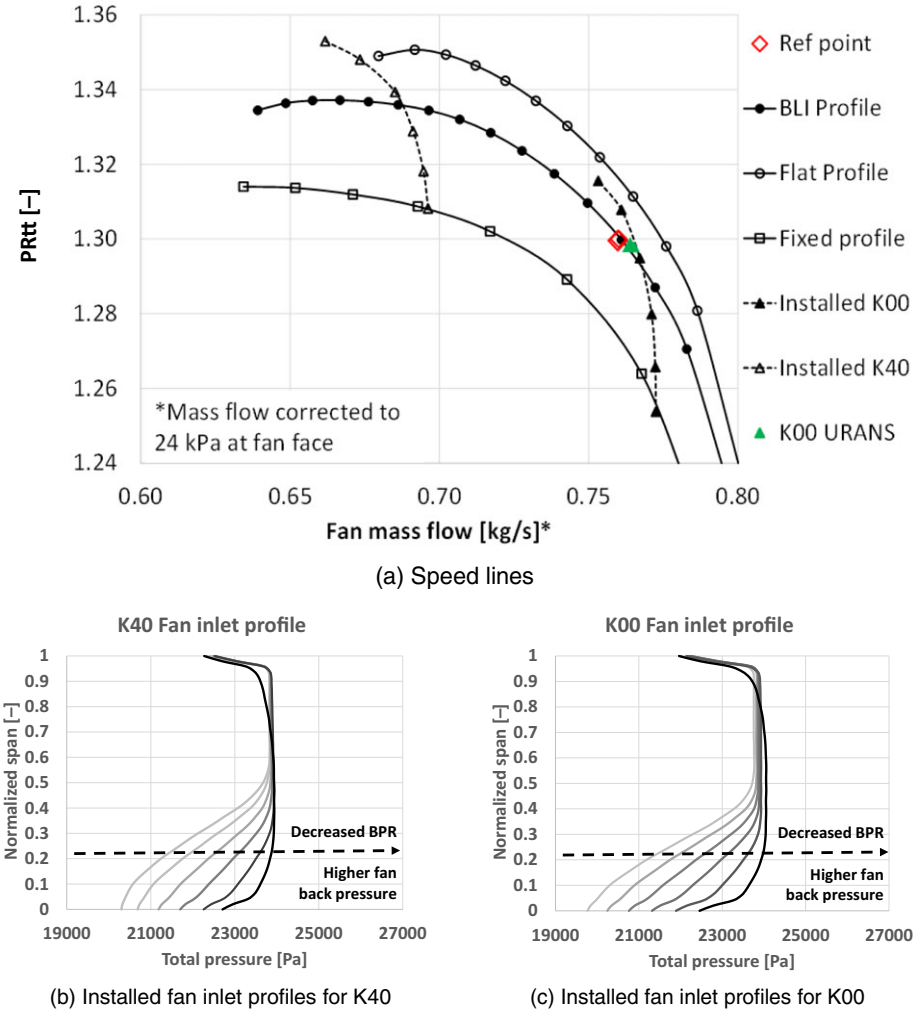

Figure 8. *Speed lines and radial profiles of total pressure.*

mass flow through the fan. In the case of "BLI Profile" this is taken from the whole aircraft analysis and is used as the reference for the design. It is therefore expected that the "BLI Profile" speed line crosses the "Installed K00" speed line near the design point. This helps to understand the effect of the installation in the rig with a by-pass flow. The "Installed K00" and "Installed K40" speed lines differ significantly from the speed lines computed using the "BLI Profile" or the "Flat Profile". All speed lines refer to the same corrected speed and would therefore be expected to behave more similarly. The reason they do not is that the inlet profile changes rapidly with the by-pass ratio in the rig. Figure 8b and 8c shows the inlet profiles for the operating points computed with the fan installed in the whole rig analyses. A striking feature is the strong increase in total pressure deficit near the hub as the mass flow increases. In Fig. 8b and 8c the circumferentially averaged radial total pressure profiles exhibit a deficit near the hub that becomes significantly larger at the higher flow rates. This is likely due to the increasing friction losses incurred on the centerbody with increased flow rate. A second effect is that with a larger by-pass the stream tube captured by the fan will have a smaller area and consist of a higher percentage of boundary layer flow. The "Flat Profile" would be the curve that installed speed lines should fall on if there is no variation of the flow ingested into the fan. The points on the profiles with low flow tend towards this as is seen

https://doi.org/10.1017/aer.2022.28 Published online by Cambridge University Press

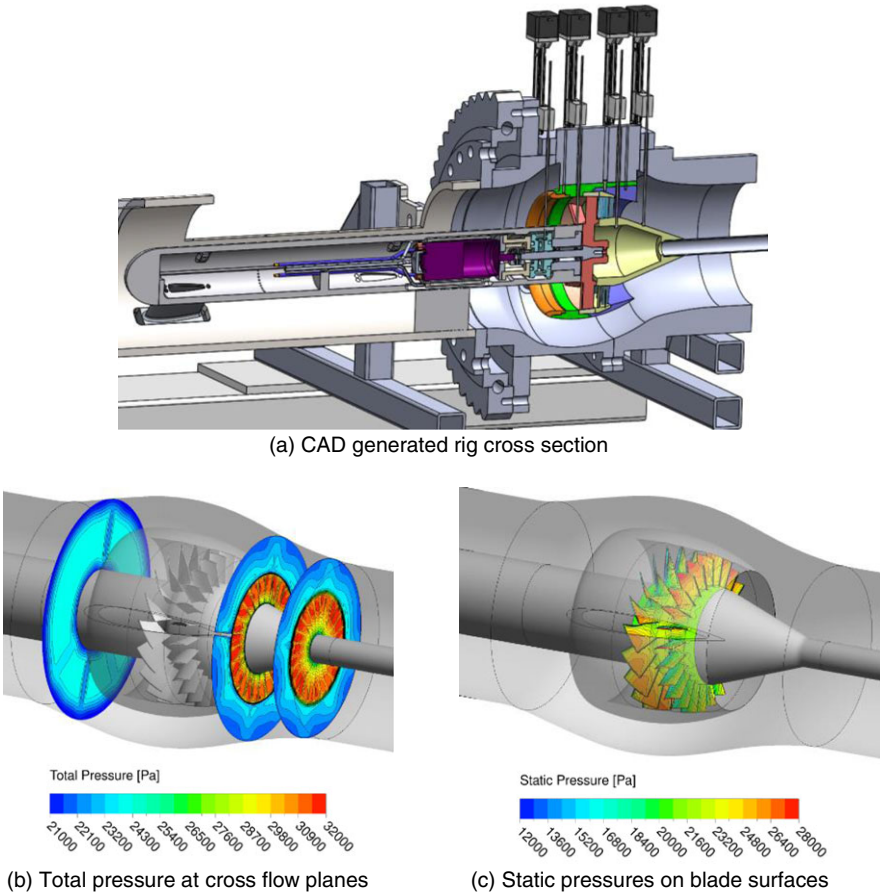

(a) CAD generated rig cross section

(b) Total pressure at cross flow planes

(c) Static pressures on blade surfaces

Figure 9. *3D overviews of rig design details (a) and snapshots of the flow in (b) and (c).*

in Fig. 8b and c. The speed line denoted "Fixed Profile" is generated using the leftmost total pressure profile in Fig. 8b, which is taken at the lowest pressure ratio operating point of the "K40 Installed" speed line in 8a. This means taking the ingested profile computed from one operating point in the rig and using it to compute a speed line with a fixed inlet profile in the same way as the "BLI Profile". Plotting the speed line generated using this gives the expected result that the point we start out from lies on the speed line but also that it behaves qualitatively as the "BLI" and "Flat" speed line families moving from choke to stall. The different evolution of the "Installed" speed lines are thus shown to be governed by changes in fan inlet flow conditions that in turn are dependent on the by-pass flow.

3.3 Unsteady analysis of the rig with a 360° fan model

With a detailed unsteady CFD model performed at the reference point, the effects of the non-axisymmetric distortion features become traceable. Figure 9a depicts a cutaway through the rig boundary layer generating body, fan and traverse systems as designed. In a small rig the absolute determination of fan efficiency from measurements will be difficult. However, the pressure mapping will be used for understanding the performance in terms of stall margin, and to understand the transfer of the distortion pattern through the fan. A total of five instrumentation traverses pass through the nacelle and will be used to map pressure, temperature and flow directionality. Axial locations include inlet to the nacelle, the fan inlet face, between the rotor and stator, immediately downstream of the stator, and at the exit

https://doi.org/10.1017/aer.2022.28 Published online by Cambridge University Press

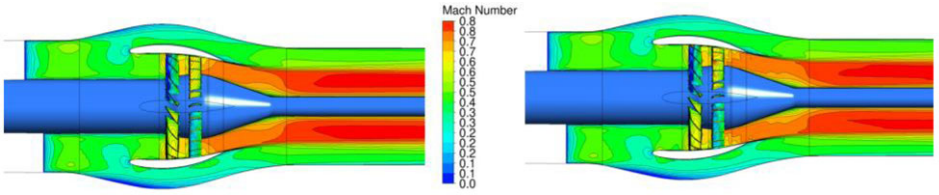

(a) Mixing planes (b) Unsteady 360 ° snapshot

Figure 10. *Flow fields from simulation.*

of the nozzle. Propagation of disturbances and the identification of rotating stall can be done by rapid pressure measurements in the fan flow path wall. CFD tools that are tested against the results of the experiment, can be used to transpose the results to full scale. Where large discrepancies are indicted, the test results are also useful to identify needs for improvement of the CFD tools. Figure 9b shows an overview of some typical station planes in the CFD model with total pressures, and Fig. 9c shows the instantaneous static pressures on blade and vane surfaces.

Comparing the results of using mixing planes to the unsteady 360° computation yields results that are in close agreement for the performance. The meshes are the same, but in the 360° model all the blades and vanes are included, repeating up the meshes for all 18 blades and 24 vanes, respectively. The simulation models the time dependent flow with the rotor moving appropriately relative to the rig. There is a possibility that the circumferential distortion would modify the behaviour of the fan, a case that the performance calculations with mixing planes would not reveal. To this point the simulations are made to confirm that the earlier used assumptions for the CFD of using mixing plane models for the fan have not been too far off. The red marked symbol in Fig. 8a denoted K00 URANS, close to the reference point identifies the result of the computation. As can be noted, it is close to the corresponding result on the K00 speed line, indicating that the overall performance is similar. At this operating point a cut through the vertical symmetry plane is taken from a simulation using mixing planes and the 360° model. Figure 10 shows the Mach number contours on a symmetry plane and surface pressures on the blades and vanes. Small variations in pressure are observed on the blades and, in particular, the vane surfaces in the unsteady simulation compared to the mixing plane case. Some differences can also be seen for the Mach number contours on the symmetry plane. In the unsteady case, the Mach numbers in the jet are not perfectly symmetric due to the asymmetry of the flow propagating through the fan. It should be noted at this point that the circumferential distortion in this baseline configuration is smaller than expected for the full-scale fan.

4.0 Conclusion

Some important aspects on the design of a BLI fan for a sub-scale rig with a by-pass duct have been covered in the current study. The main issues addressed in the design of the sub-scale fan suitable for rig testing were limitations imposed by the smaller geometric scale of the fan, facility power limitations and the integration of the fan into the rig. The design and analysis were taken in steps of increasing analytical fidelity. Firstly, aspects relating more to the size and design point performance were covered. The smaller geometric size required that blade and vane geometric shape changes were introduced to facilitate manufacturing while maintaining performance characteristics. Secondly, the installed operation of the fan, and its effects on the operating conditions for the fan were studied in order to verify that the fan will work as expected in the rig environment and be able provide for good data in the test. The by-pass flow in the rig was shown to have important effects on performance with changes in the rig throttle, where an addition of a nozzle blocker plate device was needed in order to explore higher pressure ratio fan operating points. The ingested profile found in the baseline rig configuration was different from the

https://doi.org/10.1017/aer.2022.28 Published online by Cambridge University Press

design boundary conditions from the whole aircraft CFD but was shown to contain the key ingested features. Around the intended design point the installed fan performance was similar to that found when using the design profile. This is a good result and indicates that the fan can be used to study a wide range of inlet conditions. In off-design operation, the by-pass flow was found to be sensitive to throttling of the rig, which resulted in changes of the ingested flow. The resulting change in total pressure profile of the flow was shown to have a significant effect on the fan performance. An important conclusion from this is that a separate fan nozzle blockage must be added in order to reach fan operating points approaching stall. Finally, at relatively low levels of circumferential distortion the performance was verified in an unsteady 360° simulation. This also served to demonstrate that the simpler simulations used for the design and installation have a good degree of validity, also when used with the more complex flow conditions given by the rig environment. The design and analysis effort provides knowledge of how the fan can be expected to perform installed in the rig. Understanding this is helpful in creating meaningful test that can in turn serve as a validation for the computational tools used as well as for future design efforts.

Acknowledgments. GKN Aerospace, and NRC for funding and granting permission to publish this work. NFFP, for parts of the funding. Our colleagues Simon Taylor who initiated the collaboration with great enthusiasm, Anders Sjunnesson and Fredrik Wallin who have supported the work at GKN.

References

[1] Smith, A. and Roberts, H. The jet airplane using boundary layer air for propulsion, J. Aeronaut. Sci. 1947; **14**, 2, 97–109.
[2] Smith, L.H., Jr. Wake ingestion propulsion benefit, *J. Propuls. Power*, 1993; **9**, 1, 74–82.
[3] Plas, A.P., Sargeant, M.A., Madani, V., Crichton, D., Greitzer, E.M., Hynes, T.P., Hall, C.A., Performance of a boundary layer ingesting (BLI) propulsion system, 45th AIAA Aerospace Sciences Meeting and Exhibit, 8–11 January 2007, Reno, Nevada.
[4] Drela, M. Development of the D8 transport configuration, Paper 2011-3970, 29th AIAA Applied Aerodynamics conference, 27–30 June 2011, Honolulu, HI, USA.
[5] Uranga, A., Drela, M., Greitzer, E., Titchener, N., Lieu, M., Siu, N., Huang, A., Gatlin, G., Hannon, J., Preliminary experimental assessment of the boundary layer ingestion benefit for the D8 aircraft, Proceedings of the 52nd Aerospace Sciences Meeting, AIAA SciTech Forum AIAA 2014-0906, National Harbor, MD, USA, 13–17, January 2014, doi: 10.2514/6.2014-0906.
[6] Celestina, M. and Long-Davis, M. Large-scale boundary layer ingesting propulsor research, ISABE-2019-24264, Proceedings of the 24th ISABE conference, Canberra, Australia, 2019.
[7] Welstead, J. and Felder, J. Conceptual design of a single-aisle turboelectric commercial transport with fuselage boundary layer ingestion, 54th AIAA Aerospace Sciences Meeting, doi: 10.2514/6.2016-1027, 2016.
[8] Seitz, A., Peter, F., Bijewitz, J., Habermann, A., Goraj, Z., Kowalski, M., Castillo Pardo, A., Hall, C.A., Meller, F., Merkler, R., Petit, O., Samuelsson, S., Della Corte, B., van Sluis, M., Wortmann, G. and Dietz, M. Concept validation study for fuselage wake filling propulsion integration, 31st Congress of the International Council of the Aeronautical Sciences, International Council of Aeronautical Sciences, Sept. 2018.
[9] Pardo, A. and Hall, C. Aerodynamics of boundary layer ingesting fuselage fans, ISABE-2019-24162, Proceedings of the 24th ISABE conference, Canberra, Australia, 2019.
[10] Gunn, E. and Hall, C. Aerodynamics of boundary layer ingesting fans, GT2014-26142, Proceedings of ASME Turbo Expo, 2014.
[11] Provenza, A., Duffy, K., Bakhle, M., Aeromechanical response of a distortion tolerant boundary layer ingesting fan, GT2018-77094, Proceedings of ASME Turbo Expo, 2018.
[12] Rasimarzabadi, F. Engine inlet velocity profile effects- design part, Report No.: LTR-GTL-2020-0077, National Research Council Canada, Gas Turbine Laboratory, 2020.
[13] Mårtensson, H. and Laban, M. Design and performance of a boundary layer ingestion fan. Proceedings of ASME Turbo Expo 2020 virtual conference. GT2020-15479, June 2020.
[14] Mårtensson, H., Ellbrant, L. and Lundbladh, A. Design conditions for an aft mounted fan with boundary layer ingestion, ISABE-2019-24258.
[15] Sakulkaew, S., Tan, C.S., Donahoo, E., Cornelius, C. and Montgomery, M. Compressor efficiency variation with rotor tip gap from vanishing to large clearance, *ASME. J. Turbomach.* 2013, **135**, 3, p 031030. https://doi.org/10.1115/1.4007547
[16] Copenhaver, W.W., Mayhew, E.R., Hah, C. and Wadia, A.R. The effect of tip clearance on a swept transonic compressor rotor, *ASME. J. Turbomach.* 1996; **118**, 2, 230–239. https://doi.org/10.1115/1.2836630

Cite this article: Mårtensson H., Lejon M., Ghosh D., Åkerberg M., Rasimarzabadi F. and Neuteboom M. (2022). Design of a sub-scale fan for a boundary layer ingestion test with by-pass flow. *The Aeronautical Journal*, **126**, 1288–1302. https://doi.org/10.1017/aer.2022.28